Solid State Ionics 290 (2016) 108–115

Contents lists available at ScienceDirect

Solid State Ionics

journal homepage: www.elsevier.com/locate/ssi

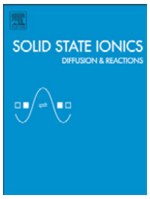

Oxygen isotope exchange in doped calcium and barium zirconates

A.S. Farlenkov [a,*], M.V. Ananyev [a,b], V.A. Eremin [a], N.M. Porotnikova [a], E.Kh. Kurumchin [a], B.-T. Melekh [c]

[a] *Institute of High Temperature Electrochemistry of the Ural Branch of the Russian Academy of Sciences, Yekaterinburg 620137, Russia*
[b] *Ural Federal University named after the first President of Russia B.N. Yeltsin, Yekaterinburg 620990, Russia*
[c] *Ioffe Physico–Technical Institute of the Russian Academy of Science, St. Petersburg 194021, Russia*

ARTICLE INFO

Article history:
Received 11 July 2015
Received in revised form 6 April 2016
Accepted 19 April 2016
Available online 27 April 2016

Keywords:
Calcium zirconate
Barium zirconate
Oxygen diffusion coefficient
Oxygen exchange coefficient
Oxygen isotope exchange

ABSTRACT

The oxygen tracer diffusion coefficient and the oxygen surface exchange coefficient were measured in $CaZr_{1-x}Sc_xO_{3-x/2}$ ($x = 0$, 0.01, 0.05) and $BaZr_{0.8}Y_{0.2}O_{2.9}$ zirconates over the temperature range of 700–900 °C and the oxygen pressure range of 0.13–6.67 kPa using the oxygen isotope exchange method with gas phase equilibration. The dependence of oxygen exchange coefficient on scandium content reduces gradually with temperature increasing, in the way that at 850 °C the oxygen exchange coefficient becomes almost independent on scandium concentration in calcium zirconates. The oxygen isotope exchange is found to be limited by the incorporation stage. Influence of grain boundaries on the oxygen diffusivity in calcium and barium zirconates is discussed.

1. Introduction

High-temperature proton conductors constitute a unique class of oxide materials possessing both protonic and oxygen-ionic conductivity in H_2 and H_2O containing atmospheres. Investigations of high-temperature proton conducting oxides based on alkali-earth zirconates have been performed rather intensively [1–10]. However, the kinetics of oxygen surface exchange of these compounds have not been studied well enough. Knowledge of the rate of the oxygen surface exchange and the oxygen tracer diffusion coefficients allows predicting its activity in oxidizing catalytic reactions. The information about the oxygen diffusivity in high-temperature proton conductors facilitates our understanding the mechanisms of water incorporation in case of the oxygen diffusion limitations.

Only few works [11–13] are known in which authors determined the oxygen surface exchange coefficients, oxygen tracer diffusion coefficients and apparent activation energy for processes of the oxygen surface exchange and the diffusion for proton conductors based on alkali-earth zirconates. The data presented in the literature does not bring to light the influence of acceptor doping and grain boundaries on the surface exchange kinetics and the oxygen diffusivity, since the results were obtained on samples with different compositions and, moreover, using different preparation techniques.

Generally, the effect of grain boundaries has been reported as blocking for perovskite both protonic and hole-type conductivity [14–16]. Blocking effect can be considered in terms of space-charge theory [17]. According to the theory grain boundaries show the prevailing view of positively charged grain boundary cores with depletion of positive defects and accumulation of negatively charge defects in the adjacent space-charge layers. Assuming that oxygen vacancies are stabilized in the grain boundary core in order to decrease its mismatch energy, these vacancies will not be easily filled, and grain interior vacancies are then selectively filled during hydration. Such a grain boundary core hydration would explain the observed difference in Schottky barrier height under wet and dry conditions [17].

The situation with blocking or enhancing effect of grain boundaries on oxygen diffusion process is not clear. In case of dry oxidative conditions with considerable hole-type conductivity it is very difficult to reveal the influence of grain boundaries on oxygen-ionic conductivity by means of only electrochemical methods. Using oxygen isotopic exchange and secondary ion mass spectroscopy (SIMS) characterization on dense $SrZrO_3$ polycrystalline materials it was shown that between 1173 K and 1473 K oxygen diffusion is not limited by surface exchange and grain boundaries are fast pathways for oxygen diffusion [12]. It was suggested that the samples might not be undoped, but contain some impurities acting as doping element.

The main purpose of the present work was to study the effect of temperature, pressure and dopant concentration on the oxygen surface exchange kinetics and the oxygen tracer diffusion coefficients in proton-conducting doped calcium and barium zirconates.

2. Experimental

Zirconium oxides, calcium carbonate, and scandium oxide were used as the initial reagents for synthesizing oxides $CaZr_{1-x}Sc_xO_{3-x/2}$

---

[*] Corresponding author.
E-mail address: a.farlenkov@yandex.ru (A.S. Farlenkov).

http://dx.doi.org/10.1016/j.ssi.2016.04.015
0167-2738/

($x = 0.00, 0.01, 0.05$) using the conventional ceramic technology; all reagents were of high purity grade. After presynthesis at 1100 °C, the obtained powders were ground and compacted in the form of tablets (diameter, ~20 mm; thickness, ~5 mm). The tablets were sintered in a rough vacuum to improve a sintering ability of samples at the temperature of 1600 °C during 3 h [10]. After sintering the oxidative annealing in air was performed at the temperature of 1200 °C during 10 h.

A sample of the yttrium doped barium zirconate $BaZr_{0.8}Y_{0.2}O_{2.9}$ was produced by the cold-crucible technique at Ioffe Institute, St.-Petersburg, Russia [18].

The X-ray powder diffraction analysis was carried out using D/MAX-2200 RIGAKU conventional diffractometer with CuK_{α}-radiation at room temperature in ambient air. According to the XRD patterns of samples are shown in Fig. 1 (a, b), all oxides were single-phase. The $BaZr_{0.8}Y_{0.2}O_{2.9}$ sample had (2 1 1) preferential crystallographic orientation with noticeable presence of grains with (1 1 0) and (2 2 0) orientation, see Fig. 1 (b), which is usual for the cold-crucible technique providing polycrystalline material.

Chemical composition of the samples was analyzed by the atomic emission spectroscopy applying iCAP 6300 ICP (Thermo Scientific, USA) and OPTIMA 4300 DV (Perkin Elmer, USA) spectrometers. According to the obtained data, the cation compositions of the samples correspond to theirs formulas.

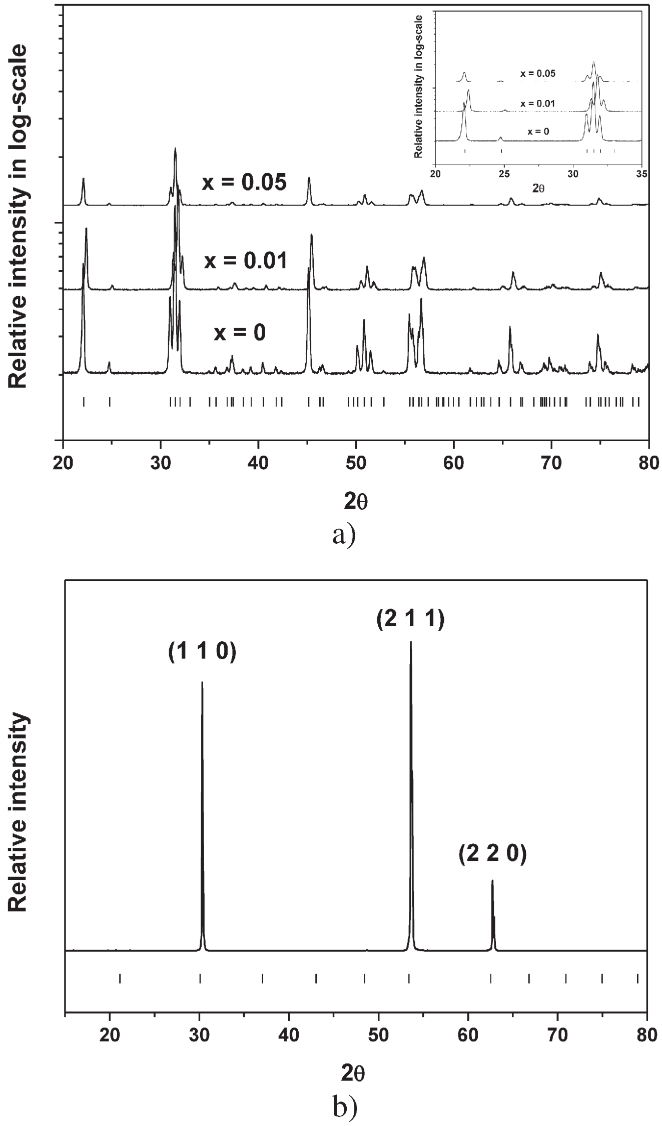

Fig. 1. XRD patterns for $CaZr_{1-x}Sc_xO_{3-x/2}$ ($x = 0, 0.01, 0.05$) and $BaZr_{0.8}Y_{0.2}O_{2.9}$.

The morphology of the samples was examined by scanning electron microscopy with Mira 3 LMU (TESCAN, Czech Republic). The microstructure of barium zirconate is totally different in comparison with calcium zirconates as shown in Fig. 2. These distinctions are caused by the different synthesis procedure. In the case of calcium zirconates the grain size is much lower in comparison with barium zirconate (0.5 mm). The mean grain diameter of calcium zirconates $CaZr_{1-x}Sc_xO_{3-x/2}$ decreases with scandium content and is equal to 6–7 μm for $CaZrO_3$, 3–4 μm for $x = 0.01$ and 2–3 μm for $x = 0.05$, see Fig. 2 (b, c, d). The SEM image processing analysis indicated that the relative density of ceramics $CaZr_{1-x}Sc_xO_{3-x/2}$ ($x = 0.00, 0.01, 0.05$) reached 96 ± 2% and $BaZr_{0.8}Y_{0.2}O_{2.9}$ reached 100%.

The oxygen isotope exchange method with gas phase equilibration was used to investigate *in situ* the interaction kinetics of oxygen from the gas phase with the samples [19]. Before experiments the surfaces of all specimens were thoroughly grinded with diamond faceplate, then polished with diamond paste and cleaned using ethyl alcohol in ultrasound bath over 1 h.

The scheme of the static circulation experimental rig is presented in Fig. 3, which consisted of reactor with the specimen (7), the gas loop with circulation pump (3), gas inlet system (6, 8, 9), turbo pumping system (5) with high vacuum ion pump (2), and the quadrupole mass-spectrometer (1). The vacuum part of the rig (Fig. 3) was made of stainless steel vacuum valves with copper and teflon ferules. The helium leakage of these links was not more than 10^{-9} std. cc/s. This means that the pressure increase within the circuit of 500 ml will not rise more than 0.6% per week of exposure.

The experimental procedure includes sample pretreatment (specimen was annealed in an atmosphere of purified oxygen of natural composition, 99.999%) to remove possible organic impurities at $T = 900$ °C and $Po_2 = 6.7$ kPa during 10 h. Then the gas was replaced with a new portion of oxygen of natural composition. After that the specimen was kept in this atmosphere at the experimental temperature and pressure until a chemical equilibrium was reached by oxygen in the oxide–gas system. The equilibration state is considered to be achieved when the oxygen pressure becomes constant in the contour. After equilibrating the reactor with the specimen, it was closed and ^{18}O-oxygen (enrichment level equal 83%) was inlet into the gas contour with the same oxygen pressure as in the reactor. The oxygen isotope exchange began when the reactor was opened. The oxygen isotope composition in the gas phase during the isotope exchange experiment was monitored by the quadrupole mass-spectrometer.

3. Results and discussion

3.1. Oxygen exchange kinetics

Oxygen isotope exchange experiments have been carried out in the temperature range between 700 and 900 °C, and oxygen pressure of 0.13–6.67 kPa. The typical time dependencies of ^{18}O-fraction and the concentrations of the oxygen molecules with three different isotopic compositions in the gas phase are presented in Fig. 4 (a, b, c, d). The obtained data is processed by using the model derived by Ezin et al. [20] on the basis of the solution by K. Klier et al. [21].

This model is the result of two solution of the following system of Eq. (1) with respective boundary and initial conditions:

$$\begin{cases} \frac{N}{S}\dot{\alpha} = r_H(\alpha_S - \alpha) \\ \frac{N}{S}\dot{y} = -ry + 2r_2(\alpha_S - \alpha)^2 \\ \dot{\alpha} = D\nabla^2\alpha \\ r = r_0 + r_1 + r_2 \end{cases} \tag{1}$$

where r_H — the heterogeneous exchange rate, S — the surface area of sample; N — the amount of oxygen in the gas phase, α — oxygen isotope ^{18}O fraction, α_s — ^{18}O-fraction at the oxide surface, y — difference